

Scattering of radio frequency waves by cylindrical blobs in the plasma edge in tokamaks

S. I. Valvis^{1†}, K. Hizanidis¹, P. Papagiannis¹, A. Papadopoulos¹, E. Glytsis¹, A. Zisis², I. G. Tigelis² and A. K. Ram³

¹School of Electrical and Computer Engineering, National Technical University of Athens, 9 Iroon Polytechniou Street, Athens 15780, GR

²Department of Physics, National and Kapodistrian University of Athens, University Campus, Zografou, Athens 15784, GR

³Plasma Science and Fusion Center, Massachusetts Institute of Technology, Cambridge MA, 175 Albany Street, Cambridge, MA 02139, USA

(Received xx; revised xx; accepted xx)

Radio frequency waves are routinely used in tokamak fusion plasmas for plasma heating, current control, and as well as in diagnostics. These waves are excited by antenna structures placed near the tokamak's wall and they have to propagate through a turbulent layer known as scrape-off layer, before reaching the core plasma (which is their target). This layer exhibits coherent density fluctuations in the form of blobs and filaments. The scattering processes of RF plane waves by single blob is studied, with the assumption that the blob has cylindrical shape and infinite length. The axis of the blob is not necessarily aligned with the externally applied magnetic field in the case of plane waves. The investigation concerns the case of Electron Cyclotron (EC) waves ($f_0=170\text{ GHz}$) for ITER-like and Medium Size Tokamak applications (such as TCV, ASDEX-U, DIII-D, etc) as well as the case of Low Hybrid (LH) waves ($f_0=4.6\text{ GHz}$) for ALCATOR C-MOD Tokamak device. The study covers for a variety of density contrasts between the blobs and the ambient plasma and a wide range of blob radii.

1. Introduction

An external antenna structure at the edge of a tokamak fusion device, excites radio frequency waves for plasma heating and plasma current generating. These waves, have to propagate through a turbulent scrape-off layer before they reach their target, which is the plasma core. The scrape-off layer consists of blobs and filaments surrounded by the ambient plasma, which differ from their background environment with respect to the plasma electrons density. As a result, the plasma permittivity of this layer's filaments is different from the background plasma's permittivity. For this reason, the characteristic properties of the incident radio frequency waves can change during their transition through the scrape-off layer, so that the RF waves are modified by the fluctuations inside it.

The study of the effects that the propagation through a different dielectric media (like blobs) has on the incident's wave properties (like electric field's intensity, Poynting vector's direction etc.) could be studied by using the geometric optics approximation. However, there is a limitation for the geometric optic's results to be valid: the electrons density of the filament n_{fila} must be near equal to the ambient electrons density n_{ambi} ,

† Email address for correspondence: jasonv@central.ntua.gr

so that the relative density contrast between the blob and the ambient electrons density is $\delta n \equiv |n_{fila} - n_{ambi}|/n_{fila} \ll 1$, which does not happen. A typical experimental range of values for δn is inside $(0.05, 1)$. So, one can understand that there is a physical reason to derive a more general approach with validity in a larger domain which of course, must include the electron densities domain of interest.

In this paper, Maxwell's equations and other mathematical tools (like Fourier transformation, Bessel functions, cylindrical vector functions, etc.) are used to derive a full-wave analytical model for the scattering process of RF waves by cylindrical density filaments. The study described, follows the study of the previous *Scattering of radio frequency waves by cylindrical density filaments in tokamak plasmas* (Ram A. K., Hizanidis K.), but has more general validity: There is no limitation for the axis of the cylindrical filament to be aligned to the externally imposed magnetic field. The magnetic field is in angle ϕ_0 with respect to the axis of the cylinder. It must be noted that for the purposes of this paper, the toroidal plasma is assumed to have a large aspect ratio, approximated by an infinitely extended slab where the filaments exist and the magnetic field is homogeneous. In addition, the axis of the cylindrical blob is assumed to have infinite length, so that the effects due to the ends of a filament of finite axial length can be ignored. Also, the thermal effects in the scrape-off layer are not taken into account, in order for the background ambient plasmas as well as the filament to be assumed cold and uniform with the permittivity being the one of a cold plasma.

Except of the larger ranges of validity for the electrons densities relative contrast between the interior and the exterior of the blob region that the full-wave model offers, there are in parallel some physical phenomena included, that the geometric optics approximation does not describe. First of all, except of refraction, in the full-wave model reflection, diffraction and shadowing are also studied. More, the fluctuations can couple power to other plasma waves (e.g. an ordinary mode wave can activate an extraordinary mode one and vice versa). In addition, the scattered waves propagate in all radial directions of the cylindrical filament and not only forward to the core, so that there are losses on the incident power.

Another assumption of different kind that is made in this study, is that the fluctuations in the scrape-off layer are static, which means that they stand still where they are. In fact, the fluctuations are moving but there is nothing wrong with the assumption that they do not move, while according to experimental results, the speed of the toroidal propagation of the fluctuations around the tokamak is about $5 \cdot 10^3$ m/s, about five orders of magnitude below the RF waves propagation speed which is nearly the well-known speed of light.

Concerning the structure of this paper and the procedure of this study, by starting from a geometrical description, the Maxwell's equations, the dispersion relation and by making a mathematical analysis with the help of some mathematical tools (like Fourier transformations, coordinate systems transformations, cylindrical vector functions, etc), the Poynting vector in the forward (to the plasma core) direction is exported. In parallel, the electric and magnetic field components as well as the Poynting vector rest components are calculated. This analytical study, is followed by a numerical one, in which the way the fluctuations affect the RF waves propagation to the core is presented. The numerical study, covers a variety of different blob radii, different magnetic field inclinations with respect to the filament axis and different relative density contrasts between the blob and the ambient electrons density. It must be also noted that, the results received from an incident radio frequency wave of O-mode are different compared to the ones from the X-mode radio frequency wave.

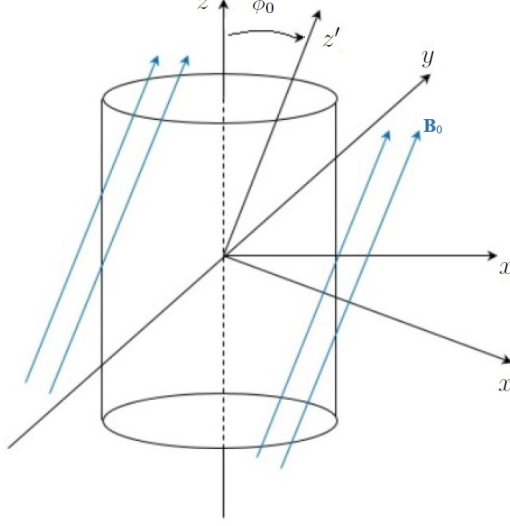


FIGURE 1. Magnetic field and cylinder coordinate systems

2. Useful formulas for the geometry

2.1. Transforming from the magnetic field coordinate system to the infinite-length cylindrical filament coordinate system

We first consider the magnetic field lines to be parallel to the $(z - x)$ -plane with z being the axis of the cylindrical blob. The cylinder has radius a and as mentioned in the introduction, is assumed to have infinite length. This assumption is acceptable, since the radius a is much smaller than its length. As a result, there are not taking place effects due to the ends of a finite-size filament. In addition, the electrons density inside the cylinder as well as the electrons density outside is considered as homogeneous and the plasma is assumed to be cold. It must be also mentioned that in this full-wave model, there is no limitation for the ratio of these two different densities.

Let ϕ_0 be the angle of the magnetic field lines (axis z') with respect to z . In order to transform between the Cartesian coordinate systems of the blob and the magnetic field one has to rotate around the fixed axis y with the help of the turning matrix

$$\overset{\leftrightarrow}{\mathbf{R}}_y(\phi_0) \equiv \begin{pmatrix} \cos \phi_0 & 0 & -\sin \phi_0 \\ 0 & 1 & 0 \\ \sin \phi_0 & 0 & \cos \phi_0 \end{pmatrix} \quad (2.1)$$

to obtain:

$$\begin{pmatrix} \hat{\mathbf{x}}' \\ \hat{\mathbf{y}}' \\ \hat{\mathbf{z}}' \end{pmatrix} = \overset{\leftrightarrow}{\mathbf{R}}_y(\phi_0) \begin{pmatrix} \hat{\mathbf{x}} \\ \hat{\mathbf{y}} \\ \hat{\mathbf{z}} \end{pmatrix}, \quad \begin{pmatrix} \hat{\mathbf{x}} \\ \hat{\mathbf{y}} \\ \hat{\mathbf{z}} \end{pmatrix} = \overset{\leftrightarrow}{\mathbf{R}}_y(-\phi_0) \begin{pmatrix} \hat{\mathbf{x}}' \\ \hat{\mathbf{y}}' \\ \hat{\mathbf{z}}' \end{pmatrix} \equiv \overset{\leftrightarrow}{\mathbf{R}}_y^{-1}(\phi_0) \begin{pmatrix} \hat{\mathbf{x}}' \\ \hat{\mathbf{y}}' \\ \hat{\mathbf{z}}' \end{pmatrix}$$

where the primed unit vectors refer to the magnetic field line coordinate system with the same y -axis. Similarly, for any vector \mathbf{a} :

$$\begin{pmatrix} a'_x \\ a'_y \\ a'_z \end{pmatrix} = \overset{\leftrightarrow}{\mathbf{R}}_y(\phi_0) \begin{pmatrix} a_x \\ a_y \\ a_z \end{pmatrix}, \quad \begin{pmatrix} a_x \\ a_y \\ a_z \end{pmatrix} = \overset{\leftrightarrow}{\mathbf{R}}_y(-\phi_0) \begin{pmatrix} a'_x \\ a'_y \\ a'_z \end{pmatrix} \equiv \overset{\leftrightarrow}{\mathbf{R}}_y^{-1}(\phi_0) \begin{pmatrix} a'_x \\ a'_y \\ a'_z \end{pmatrix}$$

and

$$\begin{pmatrix} a'_x & a'_y & a'_z \end{pmatrix} = \begin{pmatrix} a_x & a_y & a_z \end{pmatrix} \overset{\leftrightarrow}{\mathbf{R}}_y(-\phi_0) \equiv \begin{pmatrix} a_x & a_y & a_z \end{pmatrix} \overset{\leftrightarrow}{\mathbf{R}}_y^{-1}(\phi_0)$$

$$\begin{pmatrix} a_x & a_y & a_z \end{pmatrix} = \begin{pmatrix} a'_x & a'_y & a'_z \end{pmatrix} \overset{\leftrightarrow}{\mathbf{R}}_y(\phi_0)$$

2.2. Transforming from Cartesian to cylindrical coordinates and vice-versa

While being in the cylinder (blob) - based frame of reference, one can transform from cartesian coordinate system to cylindrical coordinates in the same frame. Thus, by using the transformation matrix

$$\overset{\leftrightarrow}{\mathbf{R}}_c(\varphi_k) = \begin{pmatrix} \cos \varphi_k & -\sin \varphi_k & 0 \\ \sin \varphi_k & \cos \varphi_k & 0 \\ 0 & 0 & 1 \end{pmatrix}$$

one obtains:

$$\begin{pmatrix} \hat{\mathbf{x}} \\ \hat{\mathbf{y}} \\ \hat{\mathbf{z}} \end{pmatrix} = \overset{\leftrightarrow}{\mathbf{R}}_c(\varphi_k) \begin{pmatrix} \hat{\mathbf{r}} \\ \hat{\boldsymbol{\varphi}} \\ \hat{\mathbf{z}} \end{pmatrix}, \begin{pmatrix} \hat{\mathbf{r}} \\ \hat{\boldsymbol{\varphi}} \\ \hat{\mathbf{z}} \end{pmatrix} = \overset{\leftrightarrow}{\mathbf{R}}_c(-\varphi_k) \begin{pmatrix} \hat{\mathbf{x}} \\ \hat{\mathbf{y}} \\ \hat{\mathbf{z}} \end{pmatrix} \equiv \overset{\leftrightarrow}{\mathbf{R}}_c^{-1}(\varphi_k) \begin{pmatrix} \hat{\mathbf{x}} \\ \hat{\mathbf{y}} \\ \hat{\mathbf{z}} \end{pmatrix}$$

Here, φ_k refers to the azimuthal angle in the blob-based coordinate system. Similarly, for any vector \mathbf{a} :

$$\begin{pmatrix} a_x \\ a_y \\ a_z \end{pmatrix} = \overset{\leftrightarrow}{\mathbf{R}}_c(\varphi_k) \begin{pmatrix} a_r \\ a_\varphi \\ a_z \end{pmatrix}, \begin{pmatrix} a_r \\ a_\varphi \\ a_z \end{pmatrix} = \overset{\leftrightarrow}{\mathbf{R}}_c(-\varphi_k) \begin{pmatrix} a_x \\ a_y \\ a_z \end{pmatrix} \equiv \overset{\leftrightarrow}{\mathbf{R}}_c^{-1}(\varphi_k) \begin{pmatrix} a_x \\ a_y \\ a_z \end{pmatrix}$$

and

$$\begin{pmatrix} a_x & a_y & a_z \end{pmatrix} = \begin{pmatrix} a_r & a_\varphi & a_z \end{pmatrix} \overset{\leftrightarrow}{\mathbf{R}}_c(-\varphi_k) \equiv \begin{pmatrix} a_r & a_\varphi & a_z \end{pmatrix} \overset{\leftrightarrow}{\mathbf{R}}_c^{-1}(\varphi_k)$$

$$\begin{pmatrix} a_r & a_\varphi & a_z \end{pmatrix} = \begin{pmatrix} a_x & a_y & a_z \end{pmatrix} \overset{\leftrightarrow}{\mathbf{R}}_c(\varphi_k)$$

3. Incident wave

The wavevector of the RF wave is symbolized \mathbf{k} and the radial position vector \mathbf{r} . By normalizing these two vectors to the dimensionless ones $\boldsymbol{\eta} \equiv \mathbf{k}c/\omega$ and $\boldsymbol{\rho} \equiv \mathbf{r}\omega/c$ with c being the speed of light in vacuum and $\omega = 2\pi f$ being the angular frequency (while f is the frequency). The dot product of $\boldsymbol{\eta} \cdot \boldsymbol{\rho}$ (which is the normalized $\mathbf{k} \cdot \mathbf{r}$) can be calculated in cylindrical coordinates as:

$$\begin{aligned} \boldsymbol{\eta} \cdot \boldsymbol{\rho} &= (\chi \quad \psi \quad \zeta) \begin{pmatrix} \eta_x \\ \eta_y \\ \eta_z \end{pmatrix} \\ &= (\rho \cos \varphi \quad \rho \sin \varphi \quad \zeta) \overset{\leftrightarrow}{\mathbf{R}}_c(\varphi_k) \begin{pmatrix} \eta_r \\ 0 \\ \eta_z \end{pmatrix} = \eta_r \rho \cos(\varphi - \varphi_k) + \eta_z \zeta \end{aligned}$$

where φ and φ_k are the azimuthal angles between the x -axis and $\boldsymbol{\rho}$ and $\boldsymbol{\eta}$, respectively. From now on, the subscript index "0" is used when referring to the incident wave, for which one may write:

$$\boldsymbol{\eta}_0 \cdot \boldsymbol{\rho} = \eta_{0r} \rho \cos(\varphi - \varphi_{0k}) + \eta_{0z} \zeta$$

where, now, the azimuthal angle is not in general zero. The normalized to its amplitude incident electric field intensity is:

$$\frac{\mathbf{E}_0}{E_0} \exp(i\boldsymbol{\eta}_0 \cdot \boldsymbol{\rho}) \equiv \mathbf{e}_0^P \exp\{i[\eta_{0r}\rho \cos(\varphi - \varphi_{0k} + \eta_{0z}\zeta)]\}$$

In terms of the exponential dyadic involving the vector cylinder functions \mathbf{m}_n , \mathbf{n}_n , \mathbf{l}_n in the cylinder frame of reference (convenient) one has

$$\mathbf{e}_0^P \exp(i\boldsymbol{\eta}_{0r} \cdot \boldsymbol{\rho}) = \mathbf{e}_0^P \cdot \sum_{n=-\infty}^{n=\infty} [\mathbf{a}_{0n}\mathbf{m}_n(\eta_{0r}\rho, \eta_{0z}\zeta, \varphi) + \mathbf{b}_{0n}\mathbf{n}_n(\eta_{0r}\rho, \eta_{0z}\zeta, \varphi) + \mathbf{c}_{0n}\mathbf{l}_n(\eta_{0r}\rho, \eta_{0z}\zeta, \varphi)]$$

The cylindrical vector functions in cylindrical coordinates are as follows:

$$\mathbf{m}_n(\eta_r\rho, \eta_z\zeta, \varphi) \equiv \left[in \frac{Z_n(\eta_r\rho)}{\rho} \hat{\mathbf{r}} - \frac{dZ_n(\eta_r\rho)}{d\rho} \hat{\boldsymbol{\varphi}} \right] \exp[i(\eta_z\zeta + n\varphi)]$$

$$\mathbf{n}_n(\eta_r\rho, \eta_z\zeta, \varphi) \equiv \left\{ \frac{\eta_z}{\eta} \left[i \frac{dZ_n(\eta_r\rho)}{d\rho} \hat{\mathbf{r}} - n \frac{Z_n(\eta_r\rho)}{\rho} \hat{\boldsymbol{\varphi}} \right] + \frac{\eta_r^2}{\eta} Z_n(\eta_r\rho) \hat{\boldsymbol{\zeta}} \right\} \exp[i(\eta_z\zeta + n\varphi)]$$

and

$$\mathbf{l}_n(\eta_r\rho, \eta_z\zeta, \varphi) \equiv \left[\frac{dZ_n(\eta_r\rho)}{d\rho} \hat{\mathbf{r}} + in \frac{Z_n(\eta_r\rho)}{\rho} \hat{\boldsymbol{\varphi}} + i\eta_z Z_n(\eta_r\rho) \hat{\boldsymbol{\zeta}} \right] \exp[i(\eta_z\zeta + n\varphi)]$$

Note that these vector functions are expressed in terms of the position in space (in cylindrical coordinates) while the wave enters only via its axial and radial refractive index in the cylinder frame of reference. For the incident wave the Bessel functions involved are J_n . The vector functions obey the following relations:

$$\nabla \cdot \mathbf{m}_n = 0, \quad \nabla \cdot \mathbf{n}_n = 0, \quad \nabla \cdot \mathbf{l}_n = -\eta^2 Z_n \exp[i(\eta_z\zeta + n\varphi)]$$

as well as:

$$\nabla \times \mathbf{l}_n = 0, \quad \nabla \times \mathbf{m}_n = \eta \mathbf{n}_n, \quad \nabla \times \mathbf{n}_n = \eta \mathbf{m}_n$$

3.1. Calculations of the vectors \mathbf{a}_n , \mathbf{b}_n , \mathbf{c}_n in general

Because of the completeness property of the vector cylindrical functions, the vectorial coefficients \mathbf{a}_n , \mathbf{b}_n and \mathbf{c}_n in the dyadic of the exponential can be calculated for the incident or the blob fields and the applied as well in the expressions for the scattered fields. Note that the index "k" is referring to the cylindrical filament's coordinate system. So, in the Cartesian coordinate system of the cylinder it is:

$$\begin{pmatrix} \hat{\mathbf{x}} \\ \hat{\mathbf{y}} \\ \hat{\mathbf{z}} \end{pmatrix} e^{i\boldsymbol{\rho} \cdot \boldsymbol{\eta}_k} = \sum_{n=-\infty}^{n=\infty} \left[\begin{pmatrix} a_{kn}^x \\ a_{kn}^y \\ a_{kn}^z \end{pmatrix} \mathbf{m}_n + \begin{pmatrix} b_{kn}^x \\ b_{kn}^y \\ b_{kn}^z \end{pmatrix} \mathbf{n}_n + \begin{pmatrix} c_{kn}^x \\ c_{kn}^y \\ c_{kn}^z \end{pmatrix} \mathbf{l}_n \right]$$

where after calculations, the coefficients are:

$$\begin{pmatrix} a_{kn}^x \\ a_{kn}^y \\ a_{kn}^z \end{pmatrix} = \begin{pmatrix} -\sin \varphi_k \\ \cos \varphi_k \\ 0 \end{pmatrix} \frac{i^{n+1} e^{-in\varphi_k}}{\eta_{kr}}$$

$$\begin{pmatrix} b_{kn}^x \\ b_{kn}^y \\ b_{kn}^z \end{pmatrix} = -i^n \frac{\eta_{kz}}{\eta_k \eta_{kr}} e^{-in\varphi_k} \begin{pmatrix} \cos \varphi_k \\ \sin \varphi_k \\ -\frac{\eta_{kr}}{\eta_{kz}} \end{pmatrix}$$

$$\begin{pmatrix} c_{kn}^x \\ c_{kn}^y \\ c_{kn}^z \end{pmatrix} = -i^{n+1} \frac{e^{-in\varphi_k}}{\eta_k^2} \begin{pmatrix} \eta_{kr} \cos \varphi_k \\ \eta_{kr} \sin \varphi_k \\ \eta_{kz} \end{pmatrix}$$

4. Propagation of RF waves in plasma and the dispersion relation

4.1. The electric field in general

For a cold plasma, the Faraday equation can be combined with the Ampere equation in the Fourier domain to produce the following:

$$\varepsilon_0 \nabla \times \nabla \times \mathbf{E}(\mathbf{r}) - \left(\frac{\omega}{c}\right)^2 \mathbf{D}(\mathbf{r}) = 0$$

It is assumed that the plasma equilibrium is time independent and the linearized perturbed electromagnetic fields have a time dependence of the form $e^{-i\omega t}$, with t being the time. In normalized wave vector representation:

$$\mathbf{E}(\mathbf{r}) = \int \int \int d^3\eta \mathbf{E}(\boldsymbol{\eta}) \exp(i\boldsymbol{\eta} \cdot \boldsymbol{\rho})$$

The combination of these two equations leads to:

$$\mathbf{E}(\mathbf{r}) = \int \int \int d^3\eta \overset{\leftrightarrow}{\boldsymbol{\Delta}}(\boldsymbol{\eta}) \mathbf{E}(\boldsymbol{\eta}) \exp(i\boldsymbol{\eta} \cdot \boldsymbol{\rho})$$

where the dispersion tensor $\overset{\leftrightarrow}{\boldsymbol{\Delta}}(\boldsymbol{\eta})$ appears. For non-trivial solutions for the electric field intensity, the determinant of the dispersion tensor must be zero. The latter requirement, the dispersion relation in other words, selects the sub-manifold in the Fourier space where non-trivial electric field Fourier components exist. That is:

$$\mathcal{D}(\boldsymbol{\eta}) \equiv \det \left[\overset{\leftrightarrow}{\boldsymbol{\Delta}}(\boldsymbol{\eta}) \right] = 0$$

or, in a cylindrical frame of reference for the wave vector with a z -axis aligned with the cylinder's z -axis:

$$\mathcal{D}(\eta_{kr}, \eta_{kz}, \varphi_k) = 0$$

which it turns out to be a fourth order equation with respect to η_{kr} (see in the following). Thus:

$$\mathbf{E}(\boldsymbol{\rho}) = \sum_{M=1}^4 \int_0^{2\pi} d\varphi_k \int_{-\infty}^{\infty} d\eta_{kz} \mathbf{E}_k [\eta_{kr}(\eta_{kz}, \varphi_k), \eta_{kz}, \varphi_k] \exp(i\boldsymbol{\eta}_k \cdot \boldsymbol{\rho})$$

or, equivalently:

$$\begin{aligned} \mathbf{E}(\rho, \varphi, \zeta) &= \sum_{M=1}^4 \int_0^{2\pi} d\varphi_k \int_{-\infty}^{\infty} d\eta_{kz} \mathbf{E}_k^M [\eta_{kr}^M(\eta_{kz}, \varphi_k), \eta_{kz}, \varphi_k] \\ &\quad \exp \left\{ i \left[\rho \eta_{kr}^M \cos(\varphi - \varphi_k) + \eta_{kz} \zeta \right] \right\} \end{aligned}$$

with the letter "M" referring to the number of the solution (while in general, there are four solutions for any fourth-order equation). One may introduce a factor of $\frac{1}{2\pi}$ in front of these expressions in order to relate easily back to the case of the aligned cylinder.

4.2. The dispersion relation exportation

In the magnetic field frame of reference (previously primed), in cartesian coordinates the permittivity tensor has the form:

$$\overset{\leftrightarrow}{\mathbf{K}}_{mag}^{cart} = \begin{pmatrix} K_{\perp} & -iK_{\times} & 0 \\ iK_{\times} & K_{\perp} & 0 \\ 0 & 0 & K_{\parallel} \end{pmatrix}$$

With the help of some formulas mentioned previously, the permittivity tensor can be expressed in the cylinder frame of reference, in cartesian coordinates:

$$\overset{\leftrightarrow}{\mathbf{K}}_{fila}^{cart} = \overset{\leftrightarrow}{\mathbf{R}}_y^{-1}(\phi_0) \overset{\leftrightarrow}{\mathbf{K}}_{mag}^{cart} \overset{\leftrightarrow}{\mathbf{R}}_y(\phi_0)$$

which after the calculations give:

$$\overset{\leftrightarrow}{\mathbf{K}}_{fila}^{cart} = \begin{pmatrix} K_{\perp}c_0^2 + K_{\parallel}s_0^2 & -iK_{\times}c_0 & c_0s_0(K_{\parallel} - K_{\perp}) \\ iK_{\times}c_0 & K_{\perp} & -iK_{\times}s_0 \\ c_0s_0(K_{\parallel} - K_{\perp}) & iK_{\times}s_0 & K_{\perp}s_0^2 + K_{\parallel}c_0^2 \end{pmatrix}$$

where

$$c_0 \equiv \cos \phi_0, \quad s_0 \equiv \sin \phi_0$$

It has to be emphasized, that the angle ϕ_0 is the angle between the axis of the cylindrical filament and the magnetic field line and must not be confused with the azimuthal angles in the cylindrical coordinate systems, which in general are symbolized as φ . The dispersion tensor, can be calculated from the permittivity tensor, in the same frame of reference and the same coordinate system, by using the following:

$$\overset{\leftrightarrow}{\Delta}_{fila}^{cart} = \overset{\leftrightarrow}{\mathbf{K}}_{fila}^{cart} + (\boldsymbol{\eta}\boldsymbol{\eta} - \mathbf{I}\eta^2)_{fila}^{cart}$$

So, it is obtained that:

$$\overset{\leftrightarrow}{\Delta}_{fila}^{cart} = \begin{pmatrix} K_{\perp}c_0^2 + K_{\parallel}s_0^2 - \eta_y^2 - \eta_z^2 & -iK_{\times}c_0 + \eta_x\eta_y & c_0s_0(K_{\parallel} - K_{\perp}) + \eta_x\eta_z \\ iK_{\times}c_0 + \eta_x\eta_y & K_{\perp} - \eta_x^2 - \eta_z^2 & -iK_{\times}s_0 + \eta_y\eta_z \\ c_0s_0(K_{\parallel} - K_{\perp}) + \eta_x\eta_z & iK_{\times}s_0 + \eta_y\eta_z & K_{\perp}s_0^2 + K_{\parallel}c_0^2 - \eta_x^2 - \eta_y^2 \end{pmatrix}$$

Now, in cylindrical coordinates:

$$\begin{aligned} \overset{\leftrightarrow}{\Delta}_{fila}^{cyl} &= \overset{\leftrightarrow}{\mathbf{R}}_c^{-1}(\varphi_k) \overset{\leftrightarrow}{\Delta}_{fila}^{cart} \overset{\leftrightarrow}{\mathbf{R}}_c(\varphi_k) \\ &= \overset{\leftrightarrow}{\mathbf{R}}_c^{-1}(\varphi_k) \overset{\leftrightarrow}{\mathbf{K}}_{fila}^{cart} \overset{\leftrightarrow}{\mathbf{R}}_c(\varphi_k) + \boldsymbol{\eta}_{fila}^{cyl} (\boldsymbol{\eta}_{fila}^{cyl})^T - \mathbf{I}\eta^2 \end{aligned}$$

Note now that the index in the azimuthal angle refers to a particular wave vector in a \mathbf{k} -space coordinate system with k_z component along the axis of the blob and azimuthal angle of the projection of \mathbf{k} on the $(x-y)$ plane with respect to the x -axis of the Cartesian blob-based system. In the following the azimuthal component of the \mathbf{k} -field is actually zero. Executing the multiplications renders:

$$(\Delta_{fila}^{cyl})_{11} = c_k^2(K_{\perp}c_0^2 + K_{\parallel}s_0^2) + K_{\perp}s_k^2 - \eta_{\varphi}^2 - \eta_z^2$$

$$(\Delta_{fila}^{cyl})_{12} = -s_k c_k (K_{\perp} c_0^2 + K_{\parallel} s_0^2) + K_{\perp} s_k c_k - iK_{\times} c_0 + \eta_r \eta_{\varphi}$$

$$(\Delta_{fila}^{cyl})_{13} = c_k c_0 s_0 (K_{\parallel} - K_{\perp}) - iK_{\times} s_0 s_k + \eta_r \eta_z$$

$$(\Delta_{fila}^{cyl})_{21} = -s_k c_k (K_{\perp} c_0^2 + K_{\parallel} s_0^2) + K_{\perp} s_k c_k + iK_{\times} c_0 + \eta_r \eta_{\varphi}$$

$$(\Delta_{fila}^{cyl})_{22} = s_k^2 (K_{\perp} c_0^2 + K_{\parallel} s_0^2) + K_{\perp} c_k^2 - \eta_r^2 - \eta_z^2$$

$$(\Delta_{fila}^{cyl})_{23} = -s_k c_0 s_0 (K_{\parallel} - K_{\perp}) - iK_{\times} s_0 c_k + \eta_{\varphi} \eta_z$$

$$(\Delta_{fila}^{cyl})_{31} = c_k c_0 s_0 (K_{\parallel} - K_{\perp}) + iK_{\times} s_0 s_k + \eta_r \eta_z$$

$$(\Delta_{fila}^{cyl})_{32} = -s_k c_0 s_0 (K_{\parallel} - K_{\perp}) + iK_{\times} s_0 c_k + \eta_{\varphi} \eta_z$$

$$(\Delta_{fila}^{cyl})_{33} = (K_{\perp} s_0^2 + K_{\parallel} c_0^2) - \eta_r^2 - \eta_{\varphi}^2$$

where:

$$c_k \equiv \cos \varphi_k, \quad s_k \equiv \sin \varphi_k$$

and the electric field cylindrical components satisfy the following

$$\overset{\leftrightarrow}{\Delta}_{fila}^{cyl} \begin{pmatrix} E_r \\ E_{\varphi} \\ E_z \end{pmatrix}_{fila}^{cyl} = 0$$

As it was mentioned before, the azimuthal component for the propagation vector field \mathbf{k} (the azimuthal angle φ_k suffices) is zero. Thus, the dispersion relation written down previously in the blob cylindrical frame of reference can be simplified as follows:

$$\det \left(\overset{\leftrightarrow}{\Delta}_{fila}^{cyl} \right) = 0$$

This, can be written also as:

$$\det \begin{pmatrix} Ac_k^2 + K_{\perp} s_k^2 - \eta_z^2 & (K_{\perp} - A)s_k c_k - iK_{\times} c_0 & Dc_k + \eta_r \eta_z - iK_{\times} s_0 s_k \\ (K_{\perp} - A)s_k c_k + iK_{\times} c_0 & As_k^2 + K_{\perp} c_k^2 - \eta_r^2 - \eta_z^2 & -Ds_k - iK_{\times} s_0 c_k \\ Dc_k + \eta_r \eta_z + iK_{\times} s_0 s_k & -Ds_k + iK_{\times} s_0 c_k & A' - \eta_r^2 \end{pmatrix} = 0$$

with:

$$A \equiv K_{\perp} c_0^2 + K_{\parallel} s_0^2, \quad A' \equiv K_{\perp} s_0^2 + K_{\parallel} c_0^2, \quad D \equiv (K_{\parallel} - K_{\perp}) s_0 c_0, \quad s_k \equiv \sin \varphi_k, \\ c_k \equiv \cos \varphi_k$$

which, for the incident wave [the incident wave is assumed to have the propagation vector on the $(x - z)$ -plane] becomes ($s_k = 0$, $c_k = 1$):

$$\det \begin{pmatrix} A - \eta_z^2 & -iK_{\times} c_0 & D + \eta_r \eta_z \\ iK_{\times} c_0 & K_{\perp} - \eta_r^2 - \eta_z^2 & -iK_{\times} s_0 \\ D + \eta_r \eta_z & iK_{\times} s_0 & A' - \eta_r^2 \end{pmatrix} = 0$$

Note that for any mode η_{kz} is preserved, that is, it is set by the incident one, η_{0z} . Therefore, one obtains, dropping the index "k":

$$\begin{aligned} & [K_{\perp} - (K_{\perp} - K_{\parallel})s_0^2c^2] \eta_r^4 \\ & - 2\eta_{0z}(K_{\perp} - K_{\parallel})s_0c_0c\eta_r^3 \\ & + \{(K_{\perp} + K_{\parallel})(\eta_{0z}^2 - K_{\perp}) + K_{\times}^2 + [(K_{\perp}^2 - K_{\times}^2 - K_{\perp}K_{\parallel})c^2 + \eta_{0z}^2(K_{\perp} - K_{\parallel})s^2] s_0^2\} \eta_r^2 \\ & - 2\eta_{0z} [(K_{\perp} - K_{\parallel})(\eta_{0z}^2 - K_{\perp}) + K_{\times}^2] s_0c_0c\eta_r \\ & + K_{\parallel} [(\eta_{0z}^2 - K_{\perp})^2 - K_{\times}^2] + \eta_{0z}^2 [(K_{\perp} - K_{\parallel})(\eta_{0z}^2 - K_{\perp}) + K_{\times}^2] s_0^2 = 0 \end{aligned}$$

For the incident wave in the inclined case and the propagation vector on the $z - z'$ plane (same as $x - z$ plane), that is for $c = 1$, $s = 0$, one obtains

$$\begin{aligned} & (K_{\perp}c_0^2 + K_{\parallel}s_0^2)\eta_r^4 \\ & - 2\eta_{0z}(K_{\perp} - K_{\parallel})s_0c_0\eta_r^3 \\ & + \{(K_{\perp} + K_{\parallel})(\eta_{0z}^2 - K_{\perp}) + K_{\times}^2 + (K_{\perp}^2 - K_{\times}^2 - K_{\perp}K_{\parallel})s_0^2\} \eta_r^2 \\ & - 2\eta_{0z} [(K_{\perp} - K_{\parallel})(\eta_{0z}^2 - K_{\perp}) + K_{\times}^2] s_0c_0\eta_r \\ & + K_{\parallel} [(\eta_{0z}^2 - K_{\perp})^2 - K_{\times}^2] + \eta_{0z}^2 [(K_{\perp} - K_{\parallel})(\eta_{0z}^2 - K_{\perp}) + K_{\times}^2] s_0^2 = 0 \end{aligned}$$

For the aligned cylinder and when the propagation vector is on $x - z$ plane ($s_0 = 0$, $c_0 = 1$), the corresponding equation is:

$$K_{\perp}\eta_r^4 + [(K_{\perp} + K_{\parallel})(\eta_{0z}^2 - K_{\perp}) + K_{\times}^2] \eta_r^2 + K_{\parallel} [(\eta_{0z}^2 - K_{\perp})^2 - K_{\times}^2] = 0$$

or, equivalently, introducing the polar angle, ϑ , representation:

$$\begin{aligned} & (K_{\perp} \sin^2 \vartheta + K_{\parallel} \cos^2 \vartheta) \eta_0^4 - [(K_{\perp}^2 - K_{\times}^2) \sin^2 \vartheta + (1 + \cos^2 \vartheta) K_{\perp} K_{\parallel}] \eta_0^2 \\ & + (K_{\perp}^2 - K_{\times}^2) K_{\parallel} = 0 \end{aligned}$$

which is the standard well-known form (Stix). Back in the general case, we observe that, for a fixed η_{0z} (which is preserved for an infinite cylinder along the z -axis) the equation posses four distinct roots for a particular choice of the angle φ_k , labeled $\eta_r^{(M)}$ with $M = 1, 2, 3, 4$. However, because of the presence of the cosine of the azimuthal angle in the odd order coefficients, these roots, viewed as functions of the azimuthal angle φ_k , are *symmetric* with respect to the midpoint $\varphi_k = \pi$ and *hetero-anti-symmetric* with respect to $\varphi_k = \frac{\pi}{2}$ and $\varphi_k = \frac{3\pi}{2}$. Thus, from one root function of φ_k , one may construct a second one by applying the aforementioned symmetries. We may name this pair as "*symmetry-based pair*". Since there exist four roots, there must exist two symmetry-based pairs. It is much more convenient to re-label the two pairs according to which one contains a member which coincides with the radial index of the incident wave (in the cylinder reference system). That is, one pair for the ambient environment will be labeled as O-pair (X-pair) if it contains the η_{0r} of an incident O-mode (X-mode). The respective pair for the blob parameters will retain the same characterization in order to ensure that they coincide in the limit of zero contrast (between inside and outside). The remaining pair automatically will be labeled as X-pair (O-pair). Therefore, one may introduce the indices O_1, O_2, X_1, X_2 where now O_1, O_2 and X_1, X_2 being the two symmetry-based pairs. The symmetries are as follows $M = O, X$:

$$\eta_{kr}^{M_i}(\varphi_k = 0 \rightarrow \pi) = -\eta_{kr}^{M_{3-i}}(\varphi_k = \pi \rightarrow 0)$$

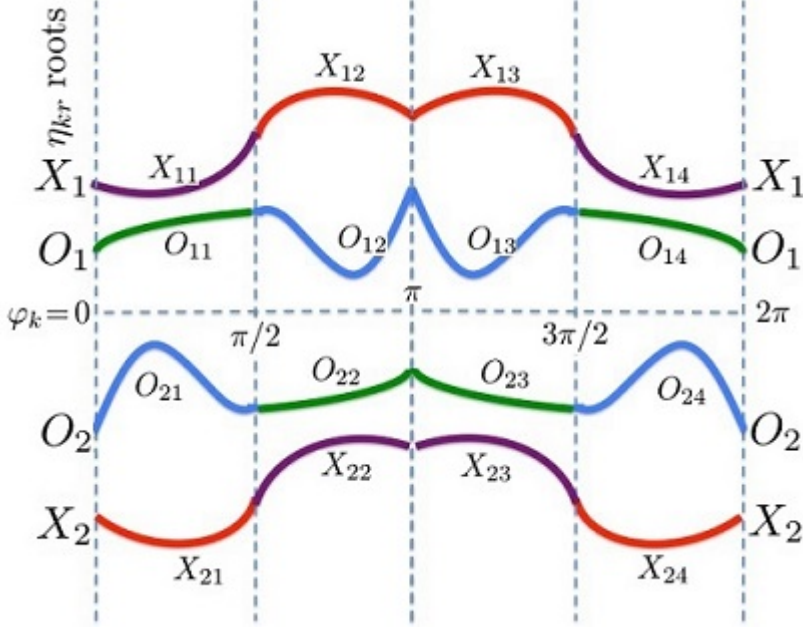


FIGURE 2. Symmetry-based pairs (O and X)

and

$$\eta_{kr}^{M_i}(\varphi_k = 0 \rightarrow \pi) = -\eta_{kr}^{M_i}(\varphi_k = 2\pi \rightarrow \pi)$$

or, equivalently:

$$\eta_{kr}^{M_i}(\varphi_k) = \eta_{kr}^{M_i}(2\pi - \varphi_k) = -\eta_{kr}^{M_{3-i}}(\pi - \varphi_k) = -\eta_{kr}^{M_{3-i}}(\pi + \varphi_k)$$

Of course, for $\varphi_k = \pi, \frac{3\pi}{2}$ the members of each pair are opposite (in the general sense). In the following, only one member of each pair will enter into play: In case of real roots only the positive (O and X) ones. In the case of imaginary roots, only the ones with positive imaginary part. And finally, for the case of complex roots (there will be two complex conjugate pairs for real η_z), the ones with positive imaginary part. These two roots are going to be used in the polarizations below.

5. Polarizations

A propagating incident wave, depending on the conditions of the ambient medium is considered to be either an O- or an X-mode (in the following the labeling "O" and "X" refer to the incident field). The homogeneous system is:

$$\begin{pmatrix} Ac^2 + K_{\perp}s^2 - \eta_{0z}^2 & (K_{\perp} - A)sc - iK_{\times}c_0 & Dc + \eta_r\eta_{0z} - iK_{\times}s_0s \\ (K_{\perp} - A)sc + iK_{\times}c_0 & As^2 + K_{\perp}c^2 - \eta_r^2 - \eta_{0z}^2 & -Ds - iK_{\times}s_0c \\ Dc + \eta_r\eta_{0z} + iK_{\times}s_0s & -Ds + iK_{\times}s_0c & A' - \eta_r^2 \end{pmatrix} \begin{pmatrix} E_r \\ E_{\varphi} \\ E_z \end{pmatrix} = 0$$

From the homogeneous system one obtains (suitable for the O-mode in the previous case of the aligned cylinder):

$$\begin{pmatrix} r_{Or}^P \\ r_{O\varphi}^P \end{pmatrix} = \begin{pmatrix} (K_{\perp}c_0^2 + K_{\parallel}s_0^2)c^2 + K_{\perp}s^2 - \eta_{0z}^2 & (K_{\perp} - K_{\parallel})s_0^2sc - iK_{\times}c_0 \\ (K_{\perp} - K_{\parallel})s_0^2sc + iK_{\times}c_0 & (K_{\perp}c_0^2 + K_{\parallel}s_0^2)s^2 + K_{\perp}c^2 - \eta^2 \end{pmatrix}^{-1} \\
\begin{pmatrix} (K_{\perp} - K_{\parallel})s_0c_0c - \eta_r\eta_{0z} + iK_{\times}s_0s \\ -(K_{\perp} - K_{\parallel})s_0c_0s + iK_{\times}s_0c \end{pmatrix} \\
r_{Oz}^P = 1$$

For the X-mode we obtain:

$$\begin{pmatrix} r_{Xr}^P \\ r_{X\varphi}^P \end{pmatrix} = \begin{pmatrix} \eta^2 - (K_{\perp}c_0^2 + K_{\parallel}s_0^2)s^2 - K_{\perp}c^2 & -(K_{\perp} - K_{\parallel})s_0c_0s + iK_{\times}s_0c \\ -(K_{\perp} - K_{\parallel})s_0c_0s - iK_{\times}s_0c & \eta_r^2 - K_{\perp}s_0^2 - K_{\parallel}c_0^2 \end{pmatrix}^{-1} \\
\begin{pmatrix} (K_{\perp} - K_{\parallel})s_0^2sc + iK_{\times}c_0 \\ \eta_r\eta_{0z} - (K_{\perp} - K_{\parallel})s_0c_0c + iK_{\times}s_0s \end{pmatrix}$$

Note that the vectorial expression for the O-mode type of polarizations is

$$\mathbf{e}_O^P \equiv \frac{E_{Oz}}{E_0}(\hat{\mathbf{k}}_r r_{Or}^P + \hat{\mathbf{k}}_{\varphi} r_{O\varphi}^P + \hat{\mathbf{k}}_z r_{Oz}^P) \equiv e_{Oz}^P \mathbf{r}_O^P$$

and respectively, for the X-mode type polarization,

$$\mathbf{e}_X^P \equiv \frac{E_{X\varphi}}{E_0}(\hat{\mathbf{k}}_r r_{Xr}^P + \hat{\mathbf{k}}_{\varphi} r_{X\varphi}^P + \hat{\mathbf{k}}_z r_{Xz}^P) \equiv e_{X\varphi}^P \mathbf{r}_X^P$$

with the hat signifying unit vectors in \mathbf{k} -space. It is useful to renormalize the polarization in such a way that leads in both cases to unitary complex vector of polarization, that is,

$$\mathbf{e}_O^P \equiv e_{Oz}^P \sqrt{\mathbf{r}_O^P \cdot (\mathbf{r}_O^P)^*} (\hat{\mathbf{k}}_r \hat{E}_{Or}^P + \hat{\mathbf{k}}_{\varphi} \hat{E}_{O\varphi}^P + \hat{\mathbf{k}}_z \hat{E}_{Oz}^P) \equiv e_{Oz}^P \sqrt{\mathbf{r}_O^P \cdot (\mathbf{r}_O^P)^*} \hat{\mathbf{E}}_O^P \equiv c_O^P \hat{\mathbf{E}}_O^P(\eta_0)$$

and

$$\mathbf{e}_X^P \equiv e_{X\varphi}^P \sqrt{\mathbf{r}_X^P \cdot (\mathbf{r}_X^P)^*} (\hat{\mathbf{k}}_r \hat{E}_{Xr}^P + \hat{\mathbf{k}}_{\varphi} \hat{E}_{X\varphi}^P + \hat{\mathbf{k}}_z \hat{E}_{Xz}^P) \equiv e_{X\varphi}^P \sqrt{\mathbf{r}_X^P \cdot (\mathbf{r}_X^P)^*} \hat{\mathbf{E}}_X^P \equiv c_X^P \hat{\mathbf{E}}_X^P(\eta_0)$$

where, by definition now:

$$\hat{\mathbf{E}}_M^P \cdot (\hat{\mathbf{E}}_M^P)^* = 1, \quad M = O, X$$

and the corresponding normalized vectorial electric field intensities \mathbf{e}_O^P and \mathbf{e}_X^P are proportional to the respective unitary complex polarization vectors via the arbitrary coefficients c_M^P (the polarization amplitudes) which are functions of the azimuthal angle and η_{0z} . Because of azimuthal symmetries described previously and the requirement of azimuthal continuity (azimuthal invariance under a rotation by π) they are related within pairs of modes (independently O or X). They are also periodic functions of the azimuthal angle. For this reason they can be written as a superposition of azimuthal modes which form a complete basis, that is:

$$c_{M_s}^P(\varphi_k, \eta_{kz}) = \sum_{n=-\infty}^{n=\infty} \varepsilon_n^{M_s}(\eta_{kz}) e^{in\varphi_k}$$

where $\varepsilon_n^{M_s}(\eta_{kz})$ are going to be determined. For the incident field we always set $c_k^P = 1$ for either O- or X-mode. We now calculate the following dot products:

$$\mathbf{e}_k^P \cdot \mathbf{a}_m, \quad \mathbf{e}_k^P \cdot \mathbf{b}_m, \quad \mathbf{e}_k^P \cdot \mathbf{c}_m; \quad k = O, X$$

that is (from known formulas for \mathbf{a}_m , \mathbf{b}_m and \mathbf{c}_m in Cartesian form expressed in terms of the radial component and the azimuth):

$$\mathbf{e}_k^P \cdot \mathbf{a}_m = c_k^P (\hat{E}_{kr}^P \hat{\mathbf{k}}_r + \hat{E}_{k\varphi_k}^P \hat{\boldsymbol{\varphi}}_k + \hat{E}_{kz}^P \hat{\mathbf{z}}) \cdot (-\hat{\mathbf{x}} \sin \varphi_k + \hat{\mathbf{y}} \cos \varphi_k) \frac{i^{m+1} \exp(-im\varphi_k)}{\eta_{kr}}$$

$$\mathbf{e}_k^P \cdot \mathbf{b}_m = -c_k^P (\hat{E}_{kr}^P \hat{\mathbf{k}}_r + \hat{E}_{k\varphi_k}^P \hat{\boldsymbol{\varphi}}_k + \hat{E}_{kz}^P \hat{\mathbf{z}}) \cdot (\hat{\mathbf{x}} \eta_{kz} \cos \varphi_k + \hat{\mathbf{y}} \eta_{kr} \sin \varphi_k - \hat{\mathbf{z}} \eta_{kr}) \frac{i^m \exp(-im\varphi_k)}{\eta_k \eta_{kr}}$$

$$\mathbf{e}_k^P \cdot \mathbf{c}_m = -c_k^P (\hat{E}_{kr}^P \hat{\mathbf{k}}_r + \hat{E}_{k\varphi_k}^P \hat{\boldsymbol{\varphi}}_k + \hat{E}_{kz}^P \hat{\mathbf{z}}) \cdot (\hat{\mathbf{x}} \eta_{kr} \cos \varphi_k + \hat{\mathbf{y}} \eta_{kr} \sin \varphi_k + \hat{\mathbf{z}} \eta_{kz}) \frac{i^{m+1} \exp(-im\varphi_k)}{\eta_k^2}$$

On the other hand, one has:

$$\begin{aligned} \hat{\mathbf{k}}_r \cdot \hat{\mathbf{x}} &= \cos \varphi_k, & \hat{\boldsymbol{\varphi}}_k \cdot \hat{\mathbf{x}} &= -\sin \varphi_k, & \hat{\mathbf{z}} \cdot \hat{\mathbf{x}} &= 0 \\ \hat{\mathbf{k}}_r \cdot \hat{\mathbf{y}} &= \sin \varphi_k, & \hat{\boldsymbol{\varphi}}_k \cdot \hat{\mathbf{y}} &= \cos \varphi_k, & \hat{\mathbf{z}} \cdot \hat{\mathbf{y}} &= 0 \\ \hat{\mathbf{k}}_r \cdot \hat{\mathbf{z}} &= 0, & \hat{\boldsymbol{\varphi}}_k \cdot \hat{\mathbf{z}} &= 0, & \hat{\mathbf{z}} \cdot \hat{\mathbf{z}} &= 1 \end{aligned}$$

Therefore:

$$\begin{aligned} \mathbf{e}_k^P \cdot \mathbf{a}_m &= c_k^P \hat{E}_{k\varphi_k}^P \frac{i^{m+1} \exp(-im\varphi_k)}{\eta_{kr}} \\ \mathbf{e}_k^P \cdot \mathbf{b}_m &= c_k^P (\hat{E}_{kz}^P \eta_{kr} - \hat{E}_{kr}^P \eta_{kz}) \frac{i^m \exp(-im\varphi_k)}{\eta_k \eta_{kr}} \\ \mathbf{e}_k^P \cdot \mathbf{c}_m &= -c_k^P (\hat{E}_{kr}^P \eta_{kr} + \hat{E}_{kz}^P \eta_{kz}) \frac{i^{m+1} \exp(-im\varphi_k)}{\eta_k^2} \end{aligned}$$

Note that for the incident wave we set the coefficients $c_k^P = 1$ and replace k by " k_0 ". Note also that in all the following, the following definition holds:

$$\eta^2 \equiv \eta_r^2 + \eta_{0z}^2$$

So, the previously obtained results are taking the form:

$$\begin{aligned} r_{Xr}^P &= 1 \\ r_{X\varphi}^P &= \frac{1}{d_X} (K_{\perp} - K_{\parallel}) \eta_r \eta_{0z} s_0 c_0 s + [K_{\times}^2 - (K_{\perp} - K_{\parallel})(K_{\perp} - \eta_r^2)] c s s_0^2 \\ &\quad - i K_{\times} [(K_{\parallel} - \eta_r^2) c_0 + \eta_r \eta_{0z} s_0 c] \\ r_{Xz}^P &= \frac{1}{d_X} (K_{\perp} - K_{\parallel}) [\eta_r \eta_{0z} s_0 s^2 + (K_{\perp} - \eta^2) c_0 c] s_0 - (K_{\perp} - \eta^2) \eta_r \eta_{0z} - K_{\times}^2 s_0 c_0 c \\ &\quad - i K_{\times} (K_{\parallel} - \eta^2) s_0 s \end{aligned}$$

where

$$\begin{aligned} d_X &\equiv -(K_{\perp} - \eta^2) \eta_r^2 - \eta^2 K_{\parallel} c_0^2 + (s^2 s_0^2 + c_0^2) K_{\perp} K_{\parallel} \\ &\quad + \{ [K_{\perp} (K_{\perp} - \eta_r^2) - K_{\times}^2] c^2 - K_{\parallel} \eta_r^2 s^2 - K_{\perp} \eta_{0z}^2 \} s_0^2 \end{aligned}$$

and

$$\begin{aligned}
r_{Or}^P &= \frac{1}{d_O} (K_\perp - K_\parallel) [\eta_r \eta_{0z} s_0 s^2 + (K_\perp - \eta^2) c_0 c] s_0 - (K_\perp - \eta^2) \eta_r \eta_{0z} - K_\times^2 c_0 s_0 c \\
&\quad + i K_\times (K_\parallel - \eta^2) s s_0 \\
r_{O\varphi}^P &= \frac{1}{d_O} \{ K_\times^2 c_0 + [\eta_r \eta_{0z} c s_0 - (K_\perp - \eta_{0z}^2) c_0] (K_\perp - K_\parallel) \} s s_0 \\
&\quad + i K_\times [(K_\parallel - \eta_{0z}^2) s_0 c + \eta_r \eta_{0z} c_0] \\
r_{Oz}^P &= 1, \\
\text{where} \\
d_O &\equiv (\eta^2 - \eta_r^2 s^2) (K_\perp - K_\parallel) s_0^2 + (K_\perp c_0^2 + K_\parallel s_0^2 - \eta^2) K_\perp - (K_\perp - \eta^2) \eta_{0z}^2 - K_\times^2 c_0^2
\end{aligned}$$

5.1. Special case: Incidence on the plane ($\mathbf{z} - \mathbf{z}'$)

In this case $s = 0$ and $c = 1$. Thus,

$$\begin{aligned}
r_{Xr}^P &= 1 \\
\begin{pmatrix} r_{X\varphi}^P \\ r_{Xz}^P \end{pmatrix} &= \begin{pmatrix} \frac{-i K_\times [(K_\parallel - \eta_r^2) c_0 + \eta_r \eta_{0z} s_0]}{(K_\perp - \eta^2) (K_\perp s_0^2 + K_\parallel c_0^2 - \eta_r^2) - K_\times s_0^2} \\ \frac{[(K_\perp - K_\parallel) (K_\perp - \eta^2) - K_\times^2] s_0 c_0 - (K_\perp - \eta^2) \eta_r \eta_{0z}}{(K_\perp - \eta^2) (K_\perp s_0^2 + K_\parallel c_0^2 - \eta_r^2) - K_\times s_0^2} \end{pmatrix}
\end{aligned}$$

and

$$\begin{aligned}
\begin{pmatrix} r_{Or}^P \\ r_{O\varphi}^P \end{pmatrix} &= \begin{pmatrix} \frac{[(K_\perp - K_\parallel) c_0 s_0 - \eta_r \eta_{0z}] (K_\perp - \eta^2) - K_\times^2 c_0 s_0}{(K_\perp^2 - K_\times^2) c_0^2 - \eta^2 (K_\perp c_0^2 + K_\parallel s_0^2) - \eta_{0z}^2 (K_\perp - \eta^2) + K_\parallel K_\perp s_0^2} \\ \frac{i K_\times [(K_\parallel - \eta_{0z}^2) s_0 + \eta_r \eta_{0z} c_0]}{(K_\perp^2 - K_\times^2) c_0^2 - \eta^2 (K_\perp c_0^2 + K_\parallel s_0^2) - \eta_{0z}^2 (K_\perp - \eta^2) + K_\parallel K_\perp s_0^2} \end{pmatrix} \\
r_{Oz}^P &= 1
\end{aligned}$$

For the aligned cylinder these boil down to:

$$\begin{pmatrix} r_{Xr}^P \\ r_{X\varphi}^P \\ r_{Xz}^P \end{pmatrix} = \begin{pmatrix} 1 \\ \frac{-i K_\times}{(K_\perp - \eta^2)} \\ \frac{-\eta_r \eta_{0z}}{K_\parallel - \eta_r^2} \end{pmatrix} \quad \text{and} \quad \begin{pmatrix} r_{Or}^P \\ r_{O\varphi}^P \\ r_{Oz}^P \end{pmatrix} = \begin{pmatrix} \frac{-\eta_r \eta_{0z} (K_\perp - \eta^2)}{(K_\perp - \eta_{0z}^2) (K_\perp - \eta^2) - K_\times^2} \\ \frac{i K_\times \eta_r \eta_{0z}}{(K_\perp - \eta_{0z}^2) (K_\perp - \eta^2) - K_\times^2} \\ 1 \end{pmatrix}$$

Note that in the aligned cylinder and for a propagation vector on the $x - z$ plane, the four roots are:

$$\begin{aligned}
\eta_r^{(\pm O)} &= \pm \frac{1}{\sqrt{2K_\perp}} \{ (K_\perp + K_\parallel) (K_\perp - \eta_{0z}^2) - K_\times^2 \\
&\quad + \sqrt{[(K_\perp - K_\parallel)^2 (K_\perp - \eta_{0z}^2) - 2K_\times^2 (K_\perp + K_\parallel)] (K_\perp - \eta_{0z}^2) + (4K_\perp K_\parallel + K_\times^2) K_\times^2} \}^{\frac{1}{2}} \\
\eta_r^{(\pm X)} &= \pm \frac{1}{\sqrt{2K_\perp}} \{ (K_\perp + K_\parallel) (K_\perp - \eta_{0z}^2) - K_\times^2 \\
&\quad - \sqrt{[(K_\perp - K_\parallel)^2 (K_\perp - \eta_{0z}^2) - 2K_\times^2 (K_\perp + K_\parallel)] (K_\perp - \eta_{0z}^2) + (4K_\perp K_\parallel + K_\times^2) K_\times^2} \}^{\frac{1}{2}}
\end{aligned}$$

that is, two O-type and two X-type. **Note that $+\mathbf{M}(-\mathbf{M})$ corresponds to $\mathbf{M}_1(\mathbf{M}_2)$ with $\mathbf{M} = \mathbf{O}, \mathbf{X}$.** Therefore, each pair consists of two opposite complex roots in general. From these pairs emanate the four roots in the inclined cylinder case that cease to form pairs as before but they are close to forming pairs as the inclination approaches zero. However, the four roots as functions of the azimuthal angle form "symmetry-based pairs" as we have shown before. In the following we may continue labeling the roots as O-type and X-type according to which type they fall to as the inclination goes to zero. For the field-aligned cylinder and the propagation vector on the $x-z$ plane one can easily observe that:

$$\begin{pmatrix} r_{X\varphi}^P(-\eta_r) \\ r_{Xz}^P(-\eta_r) \end{pmatrix} = \begin{pmatrix} r_{X\varphi}^P(\eta_r) \\ -r_{Xz}^P(\eta_r) \end{pmatrix}, \quad \begin{pmatrix} r_{Or}^P(-\eta_r) \\ r_{O\varphi}^P(-\eta_r) \end{pmatrix} = \begin{pmatrix} -r_{Or}^P(\eta_r) \\ -r_{O\varphi}^P(\eta_r) \end{pmatrix}$$

In the general case, on the other hand, we have shown that

$$\eta_{kr}^{M_i}(\varphi_k) = \eta_{kr}^{M_i}(2\pi - \varphi_k) = -\eta_{kr}^{M_{3-i}}(\pi - \varphi_k)$$

but nothing can be said as a general statement for the symmetries of the polarizations as functions of the azimuthal angle; unless, of course, the roots η_r are all real (or, purely imaginary). In the following only one member of each pair will enter into play: In case of real roots only the positive (O and X ones). In the case of imaginary roots only the ones with positive imaginary part. And, finally, for the case of complex roots (there will be two complex conjugate pairs for real η_z) the ones with positive imaginary part.

6. Back to the field expressions

Normalizing the previously found general expression for the electric field, one obtains:

$$\begin{aligned} \mathbf{e}(\mathbf{r}) &= \frac{\mathbf{E}(\mathbf{r})}{E_0} \\ &= \int_0^{2\pi} d\varphi_k \int_{-\infty}^{\infty} d\eta_{kz} \\ &\quad \sum_{M=O,X} \left\{ \mathbf{e}_k^M[\eta_{kr}^M(\varphi_k, \eta_{kz}), \varphi_k, \eta_{kz}] + \mathbf{e}_k^M[-\eta_{kr}^M(\varphi_k, \eta_{kz}), \varphi_k, \eta_{kz}] \right\} e^{i\eta_{kr}^M \rho \cos(\varphi - \varphi_k) + i\eta_{kz} \zeta} \end{aligned}$$

where the eigenmodes under the integral sign are piece-wise spatially constant. For the incident field on the other hand,

$$\mathbf{e}_0(\mathbf{r}) = \frac{\mathbf{E}_0(\mathbf{r})}{E_0} = \mathbf{e}_0(\varphi_0, \eta_{0z}) e^{i\eta_{0r} \rho \cos(\varphi - \varphi_0) + i\eta_{0z} \zeta}$$

In terms of the cylindrical vector functions and the exponential dyadic, we have:

$$\begin{aligned} &\mathbf{e}_k^M[\eta_{kr}^M(\varphi_k, \eta_{kz}), \varphi_k, \eta_{kz}] e^{i\eta_{kr}^M \rho \cos(\varphi - \varphi_k) + i\eta_{kz} \zeta} = \\ &\quad \sum_{m=-\infty}^{m=\infty} \left\{ \mathbf{e}_k^M[\eta_{kr}^M(\varphi_k, \eta_{kz}), \varphi_k, \eta_{kz}] \cdot \mathbf{a}_m[\eta_{kr}^M(\varphi_k, \eta_{kz}), \varphi_k, \eta_{kz}] \mathbf{m}_m[\rho\eta_{kr}^M(\varphi_k, \eta_{kz}), \varphi, \zeta\eta_{kz}] \right. \\ &\quad + \mathbf{e}_k^M[\eta_{kr}^M(\varphi_k, \eta_{kz}), \varphi_k, \eta_{kz}] \cdot \mathbf{b}_m[\eta_{kr}^M(\varphi_k, \eta_{kz}), \varphi_k, \eta_{kz}] \mathbf{n}_m[\rho\eta_{kr}^M(\varphi_k, \eta_{kz}), \varphi, \zeta\eta_{kz}] \\ &\quad \left. + \mathbf{e}_k^M[\eta_{kr}^M(\varphi_k, \eta_{kz}), \varphi_k, \eta_{kz}] \cdot \mathbf{c}_m[\eta_{kr}^M(\varphi_k, \eta_{kz}), \varphi_k, \eta_{kz}] \mathbf{l}_m[\rho\eta_{kr}^M(\varphi_k, \eta_{kz}), \varphi, \zeta\eta_{kz}] \right\} \end{aligned}$$

and respectively, for the incident field:

$$\begin{aligned} \mathbf{e}_0(\eta_{0r}, \eta_{0z}, \varphi_0), e^{i\eta_{0r}\rho \cos(\varphi - \varphi_0) + i\eta_{0z}\zeta} = \\ \sum_{m=-\infty}^{m=\infty} \{ \mathbf{e}_0(\eta_{0r}, \eta_{0z}, \varphi_0) \cdot \mathbf{a}_m(\eta_{0r}, \eta_{0z}, \varphi_0) \mathbf{m}_m(\rho\eta_{0r}, \eta_{0z}\zeta, \varphi_0) \\ + \mathbf{e}_0(\eta_{0r}, \eta_{0z}, \varphi_0) \cdot \mathbf{b}_m(\eta_{0r}, \eta_{0z}, \varphi_0) \mathbf{n}_m(\rho\eta_{0r}, \eta_{0z}\zeta, \varphi_0) \\ + \mathbf{e}_0(\eta_{0r}, \eta_{0z}, \varphi_0) \cdot \mathbf{c}_m(\eta_{0r}, \eta_{0z}, \varphi_0) \mathbf{l}_m(\rho\eta_{0r}, \eta_{0z}\zeta, \varphi_0) \} \end{aligned}$$

However,

$$\begin{aligned} \mathbf{e}_k^M[\eta_{kr}^M(\varphi_k, \eta_{kz}), \varphi_k, \eta_{kz}] &= c_M^P(\varphi_k, \eta_{kz}) \hat{\mathbf{E}}_M^P[\eta_{kr}^M(\varphi_k, \eta_{kz}), \varphi_k, \eta_{kz}] \\ &= \sum_{n=-\infty}^{n=\infty} \varepsilon_n^M(\eta_{kz}) e^{in\varphi_k} \hat{\mathbf{E}}_M^P[\eta_{kr}^M(\varphi_k, \eta_{kz}), \varphi_k, \eta_{kz}] \end{aligned}$$

Note that for the aligned cylinder the polarizations and the radial component of the propagation vector do not explicitly depend on the azimuthal angle. From previous calculations we have in Cartesian form:

$$\begin{aligned} \mathbf{a}_m &= i^{m+1} \frac{e^{-im\varphi_k}}{\eta_{kr}} \begin{pmatrix} -\sin \varphi_k \\ \cos \varphi_k \\ 0 \end{pmatrix}, \quad \mathbf{b}_m = -i^m \frac{\eta_{kz} e^{im\varphi_k}}{\eta_k \eta_{kr}} \begin{pmatrix} \cos \varphi_k \\ \sin \varphi_k \\ -\frac{\eta_{kr}}{\eta_{kz}} \end{pmatrix}, \\ \mathbf{c}_m &= -i^{m+1} \frac{e^{-im\varphi_k}}{\eta_{kr}^2} \begin{pmatrix} \eta_{kr} \cos \varphi_k \\ \eta_{kr} \sin \varphi_k \\ \eta_{kz} \end{pmatrix} \end{aligned}$$

Introducing the formulas for the inner products as well as the azimuthal expansion of the polarization amplitudes, one obtains in normalized form:

$$\begin{aligned} \mathbf{e}(\mathbf{r}) &= \sum_{m=-\infty}^{m=\infty} i^m \int_0^{2\pi} d\varphi_k \int_{-\infty}^{\infty} d\eta_{kz} \sum_{M=O,X} \sum_{n=-\infty}^{n=\infty} \varepsilon_n^M(\eta_{kz}) e^{i(n-m)\varphi_k} \\ &\quad \left\{ i \frac{\hat{E}_{kr}^M}{\eta_{kr}^M} \mathbf{m}_m(\rho\eta_{kr}^M, \varphi, \zeta\eta_{kz}) + \frac{\hat{E}_{kz}^M \eta_{kr}^M - \hat{E}_{kr}^M \eta_{kz}}{\eta_{kr}^M \eta_k^M} \mathbf{n}_m(\rho\eta_{kr}^M, \varphi, \zeta\eta_{kz}) \right. \\ &\quad \left. - i \frac{\hat{E}_{kr}^M \eta_{kr}^M + \hat{E}_{kz}^M \eta_{kz}}{(\eta_k^M)^2} \mathbf{l}_m(\rho\eta_{kr}^M, \varphi, \zeta\eta_{kz}) \right\} \end{aligned}$$

For the incident,

$$\begin{aligned} \mathbf{e}_0(\mathbf{r}) &= \sum_{m=-\infty}^{m=\infty} i^m e^{-im\varphi_0} \left\{ i \frac{\hat{E}_{0\varphi_0}}{\eta_{0r}} \mathbf{m}_m(\rho\eta_{0r}, \varphi, \zeta\eta_{0z}) + \frac{\hat{E}_{0z}\eta_{0r} - \hat{E}_{0r}\eta_{0z}}{\eta_{0r}\eta_0} \mathbf{n}_m(\rho\eta_{0r}, \varphi, \zeta\eta_{0z}) \right. \\ &\quad \left. - i \frac{\hat{E}_{0r}\eta_{0r} + \hat{E}_{0z}\eta_{0z}}{\eta_0^2} \mathbf{l}_m(\rho\eta_{0r}, \varphi, \zeta\eta_{0z}) \right\} \end{aligned}$$

Notice that for the aligned cylinder the mode selection does not depend on the azimuthal angle and therefore, the integration over that angle will facilitate the application of orthogonality condition for the azimuthal dependence. The magnetic field can also be easily evaluated from Faraday's law:

$$\mathbf{h} \equiv \frac{\mathbf{H}}{\mathcal{H}_0} = \frac{\mathcal{E}_0}{\mathcal{H}_0} \sqrt{\frac{\varepsilon_0}{\mu_0}} \frac{1}{i} \nabla \times \mathbf{e}, \quad \mathbf{h}_0 \equiv \frac{\mathbf{H}_0}{\mathcal{H}_0} = \frac{\mathcal{E}_0}{\mathcal{H}_0} \sqrt{\frac{\varepsilon_0}{\mu_0}} \frac{1}{i} \nabla \times \mathbf{e}_0$$

Therefore:

$$\mathbf{h}(\mathbf{r}) = \frac{E_0}{H_0} \sqrt{\frac{\varepsilon_0}{\mu_0}} \sum_{m=-\infty}^{m=\infty} i^m \int_0^{2\pi} d\varphi_k \int_{-\infty}^{\infty} d\eta_{kz} \sum_{n=-\infty}^{n=\infty} \sum_{M=O,X} \varepsilon_n^M(\eta_{kz}) e^{i(n-m)\varphi_k} \left\{ \frac{\hat{E}_{k\varphi_k}^M}{\eta_{kr}^M} \eta_k^M \mathbf{n}_m(\rho\eta_{kr}^M, \varphi, \zeta\eta_{kz}) - i \frac{\hat{E}_{kz}^M \eta_{kr}^M - \hat{E}_{kr}^M \eta_{kz}}{\eta_{kr}^M} \mathbf{m}_m(\rho\eta_{kr}^M, \varphi, \zeta\eta_{kz}) \right\}$$

and for the incident

$$\mathbf{h}_0(\mathbf{r}) = \frac{E_0}{H_0} \sqrt{\frac{\varepsilon_0}{\mu_0}} \sum_{m=-\infty}^{m=\infty} i^m e^{-im\varphi_0} \left\{ \frac{\hat{E}_{0\varphi_0}}{\eta_{0r}} \eta_0 \mathbf{n}_m(\rho\eta_{0r}, \varphi, \zeta\eta_{0z}) - i \frac{\hat{E}_{0z}\eta_{0r} - \hat{E}_{0r}\eta_{0z}}{\eta_{0r}} \mathbf{m}_m(\rho\eta_{0r}, \varphi, \zeta\eta_{0z}) \right\}$$

7. Boundary conditions

The vectorial ones are:

$$\hat{\mathbf{r}} \times (\mathbf{e}_{SC} + \mathbf{e}_0 - \mathbf{e}_{BL}) = 0, \quad \hat{\mathbf{r}} \times (\mathbf{h}_{SC} + \mathbf{h}_0 - \mathbf{h}_{BL}) = 0$$

where SC and BL stand for the exterior and the interior of the blob respectively. One can easily express the exterior products involved in the boundary conditions solely in terms of the vector functions and the tangential dyadics of unit vectors: $\hat{\mathbf{z}}\hat{\mathbf{r}}$ and $\hat{\varphi}\hat{\mathbf{z}}$:

$$\begin{aligned} \hat{\mathbf{r}} \times \mathbf{m}_m &= i(\hat{\mathbf{z}}\hat{\mathbf{r}}) \cdot \mathbf{n}_m \frac{\eta_k}{\eta_{kz}} \\ \hat{\mathbf{r}} \times \mathbf{n}_m &= i(\hat{\mathbf{z}}\hat{\mathbf{r}}) \cdot \mathbf{m}_m \frac{\eta_{kz}}{\eta_k} - (\hat{\varphi}\hat{\mathbf{z}}) \cdot \mathbf{n}_m \\ \hat{\mathbf{r}} \times \mathbf{l}_m &= (\hat{\mathbf{z}}\hat{\mathbf{r}}) \cdot \mathbf{m}_m - i(\hat{\varphi}\hat{\mathbf{z}}) \cdot \mathbf{n}_m \frac{\eta_k \eta_{kz}}{\eta_{kr}^2} \end{aligned}$$

The vector functions are calculated at a (the normalized radius of the cylinder) and the tangential components of the electric field are matched. By truncating the summation over n and writing down the conditions for the azimuthal modes, that is for each m with $m = -n_{max}$ to $m = n_{max}$, we obtain the following linear system to be solved:

$$\sum_{n=-n_{max}}^{n=n_{max}} \left(a_{j,mn}^{O,BL} \varepsilon_n^{O,BL} + a_{j,mn}^{X,BL} \varepsilon_n^{X,BL} - a_{j,mn}^{O,SC} \varepsilon_n^{O,SC} - a_{j,mn}^{X,SC} \varepsilon_n^{X,SC} \right) = a_{j,m}^0, \\ j = 1, 2, 3, 4$$

with:

$$\begin{aligned}
a_{1,mn}^{M,BL} &= \int_0^{2\pi} \frac{d\varphi_k}{2\pi} e^{i(n-m)\varphi_k} \left(i\hat{E}_{k\varphi_k}^M J_m'^M - \hat{E}_{kr}^M \frac{mJ_m^M}{\eta_{kr}^M} \right), \\
a_{1,mn}^{M,SC} &= \int_0^{2\pi} \frac{d\varphi_k}{2\pi} e^{i(n-m)\varphi_k} \left(i\hat{E}_{k\varphi_k}^M H_m'^{(1)M} - \hat{E}_{kr}^M \frac{mH_m^{(1)M}}{\eta_{kr}^M} \right), \\
a_{1,m}^0 &= e^{-im\varphi_0} \left(i\hat{E}_{0\varphi_0} J_m'^0 - \hat{E}_{0r} \frac{mJ_m^0}{\eta_{0r}} \right) \\
a_{2,mn}^{M,BL} &= \int_0^{2\pi} \frac{d\varphi_k}{2\pi} e^{i(n-m)\varphi_k} \left(\hat{E}_{kz}^M J_m^M \right), \quad a_{2,mn}^{M,SC} = \int_0^{2\pi} \frac{d\varphi_k}{2\pi} e^{i(n-m)\varphi_k} \left(\hat{E}_{kz}^M H_m^{(1)M} \right), \\
a_{2,m}^0 &= e^{-im\varphi_0} \left(\hat{E}_{0z} J_m^0 \right) \\
a_{3,mn}^{M,BL} &= \int_0^{2\pi} \frac{d\varphi_k}{2\pi} e^{i(n-m)\varphi_k} \left[i \left(\hat{E}_{kz}^M \eta_{kr}^M - \hat{E}_{kr}^M \eta_{0z} \right) J_m'^M - \hat{E}_{k\varphi_k}^M \eta_{0z} \frac{mJ_m^M}{\eta_{kr}^M} \right], \\
a_{3,mn}^{M,SC} &= \int_0^{2\pi} \frac{d\varphi_k}{2\pi} e^{i(n-m)\varphi_k} \left[i \left(\hat{E}_{kz}^M \eta_{kr}^M - \hat{E}_{kr}^M \eta_{0z} \right) H_m'^{(1)M} - \hat{E}_{k\varphi_k}^M \eta_{0z} \frac{mH_m^{(1)M}}{\eta_{kr}^M} \right], \\
a_{3,m}^0 &= e^{-im\varphi_0} \left[i \left(\hat{E}_{0z} \eta_{0r} - \hat{E}_{0r} \eta_{0z} \right) J_m'^0 - \hat{E}_{0\varphi_0} \eta_{0z} \frac{mJ_m^0}{\eta_{0r}} \right], \\
a_{4,mn}^{M,BL} &= \int_0^{2\pi} \frac{d\varphi_k}{2\pi} e^{i(n-m)\varphi_k} \left(\hat{E}_{k\varphi_k}^M \eta_{kr}^M J_m^M \right), \\
a_{4,mn}^{M,SC} &= \int_0^{2\pi} \frac{d\varphi_k}{2\pi} e^{i(n-m)\varphi_k} \left(\hat{E}_{k\varphi_k}^M \eta_{kr}^M H_m^{(1)M} \right), \quad a_{4,m}^0 = e^{-im\varphi_0} \left(\hat{E}_{0\varphi_0} \eta_{0r} J_m^0 \right)
\end{aligned}$$

8. EM fields and Poynting vector

8.1. Synthesizing the fields at arbitrary z

Integrating out the z dependence (denoted by the tilde over the vector functions), one obtains for the $(x-y)$ plane:

$$\begin{aligned}
\tilde{\mathbf{e}}(\rho, \varphi)_{(BL, SC)} &= \sum_{m=-\infty}^{m=\infty} i^m \int_0^{2\pi} d\varphi_k \sum_{M=O, X} \sum_{n=-\infty}^{n=\infty} \varepsilon_n^{M, (BL, SC)} e^{i(n-m)\varphi_k} \\
&\left[i \frac{\hat{E}_{k\varphi_k}^M}{\eta_{kr}^M} \tilde{\mathbf{m}}_m(\rho \eta_{kr}^M, \varphi) + \frac{\hat{E}_{kz}^M \eta_{kr}^M - \hat{E}_{kr}^M \eta_{0z}}{\eta_{kr}^M \eta_k^M} \tilde{\mathbf{n}}_m(\rho \eta_{kr}^M, \varphi) \right. \\
&\left. - i \frac{\hat{E}_{kr}^M \eta_{kr}^M + \hat{E}_{kz}^M \eta_{0z}}{(\eta_k^M)^2} \tilde{\mathbf{l}}_m(\rho \eta_{kr}^M, \varphi) \right]_{(BL, SC)} \\
\tilde{\mathbf{h}}(\rho, \varphi)_{(BL, SC)} &= \frac{E_0}{H_0} \sqrt{\frac{\varepsilon_0}{\mu_0}} \sum_{m=-\infty}^{m=\infty} i^m \int_0^{2\pi} d\varphi_k \sum_{M=O, X} \sum_{n=-\infty}^{n=\infty} \varepsilon_n^{M, (BL, SC)} e^{i(n-m)\varphi_k} \\
&\left[\frac{\hat{E}_{k\varphi_k}^M}{\eta_{kr}^M} \eta_k^M \tilde{\mathbf{n}}_m(\rho \eta_{kr}^M, \varphi) - i \frac{\hat{E}_{kz}^M \eta_{kr}^M - \hat{E}_{kr}^M \eta_{0z}}{\eta_{kr}^M} \tilde{\mathbf{m}}_m(\rho \eta_{kr}^M, \varphi) \right]_{(BL, SC)}
\end{aligned}$$

Respectively for the incident field:

$$\begin{aligned}\tilde{\mathbf{e}}_0(\rho, \varphi) &= \sum_{m=-\infty}^{m=\infty} i^m e^{-im\varphi_0} \\ &\left[i \frac{\hat{E}_{0\varphi_0}}{\eta_{0r}} \eta_k^M \tilde{\mathbf{m}}_m(\rho\eta_{0r}, \varphi) + \frac{\hat{E}_{0z}\eta_{0r} - \hat{E}_{0r}\eta_{0z}}{\eta_{0r}\eta_0} \tilde{\mathbf{n}}_m(\rho\eta_{0r}, \varphi) - i \frac{\hat{E}_{0r}\eta_{0r} + \hat{E}_{0z}\eta_{0z}}{\eta_0^2} \tilde{\mathbf{l}}_m(\rho\eta_{0r}, \varphi) \right] \\ \tilde{\mathbf{h}}_0(\rho, \varphi) &= \frac{E_0}{H_0} \sqrt{\frac{\varepsilon_0}{\mu_0}} \sum_{m=-\infty}^{m=\infty} i^m e^{-im\varphi_0} \\ &\left[\frac{\hat{E}_{0\varphi_0}}{\eta_{0r}} \eta_0 \tilde{\mathbf{n}}_m(\rho\eta_{0r}, \varphi) - i \frac{\hat{E}_{0z}\eta_{0r} - \hat{E}_{0r}\eta_{0z}}{\eta_{0r}} \tilde{\mathbf{m}}_m(\rho\eta_{0r}, \varphi) \right]\end{aligned}$$

By introducing the respective expressions for the vector cylinder functions, one obtains:

$$\begin{aligned}\tilde{\mathbf{e}}(\rho, \varphi)_{(BL, SC)} &= \sum_{m=-\infty}^{m=\infty} i^m e^{im\varphi} \int_0^{2\pi} d\varphi_k \sum_{M=O, X} \sum_{n=-\infty}^{n=\infty} \varepsilon_n^{M, (BL, SC)} e^{i(n-m)\varphi_k} \\ &\left[- \left(\hat{E}_{k\varphi_k}^M \frac{mZ_m^M}{\eta_{kr}^M \rho} + i \hat{E}_{kr}^M Z_m'^M \right) \hat{\mathbf{r}} + \left(\hat{E}_{kr}^M \frac{mZ_m^M}{\eta_{kr}^M \rho} - i \hat{E}_{k\varphi_k}^M Z_m'^M \right) \hat{\varphi} + \hat{E}_{kz}^M Z_m^M \hat{\mathbf{z}} \right]_{(BL, SC)} \\ \tilde{\mathbf{h}}(\rho, \varphi)_{(BL, SC)} &= \frac{E_0}{H_0} \sqrt{\frac{\varepsilon_0}{\mu_0}} \sum_{m=-\infty}^{m=\infty} i^m e^{im\varphi} \int_0^{2\pi} d\varphi_k \sum_{M=O, X} \sum_{n=-\infty}^{n=\infty} \varepsilon_n^{M, (BL, SC)} e^{i(n-m)\varphi_k} \\ &\left\{ \left[i \hat{E}_{k\varphi_k}^M \eta_{0z} Z_m'^M + \left(\hat{E}_{kz}^M \eta_{kr}^M - \hat{E}_{kr}^M \eta_{0z} \right) \frac{mZ_m^M}{\eta_{kr}^M \rho} \right] \hat{\mathbf{r}} \right. \\ &\quad \left. + \left[i \left(\hat{E}_{kz}^M \eta_{kr}^M - \hat{E}_{kr}^M \eta_{0z} \right) Z_m'^M - \hat{E}_{k\varphi_k}^M \eta_{0z} \frac{mZ_m^M}{\eta_{kr}^M \rho} \right] \hat{\varphi} + \hat{E}_{k\varphi_k}^M \eta_{kr}^M Z_m^M \hat{\mathbf{z}} \right\}_{(BL, SC)}\end{aligned}$$

Respectively for the incident field:

$$\begin{aligned}\tilde{\mathbf{e}}_0(\rho, \varphi) &= \sum_{m=-\infty}^{m=\infty} i^m e^{im(\varphi - \varphi_0)} \\ &\left[- \left(\hat{E}_{0\varphi_0} \frac{mJ_m^0}{\eta_{0r}\rho} + i \hat{E}_{0r} J_m'^0 \right) \hat{\mathbf{r}} + \left(\hat{E}_{0r} \frac{mJ_m^0}{\eta_{0r}\rho} - i \hat{E}_{0\varphi_0} J_m'^0 \right) \hat{\varphi} + \hat{E}_{0z} J_m^0 \hat{\mathbf{z}} \right] \\ \tilde{\mathbf{h}}_0(\rho, \varphi) &= \frac{E_0}{H_0} \sqrt{\frac{\varepsilon_0}{\mu_0}} \sum_{m=-\infty}^{m=\infty} i^m e^{im(\varphi - \varphi_0)} \left\{ \left[i \hat{E}_{0\varphi_0} \eta_{0z} J_m'^0 + \left(\hat{E}_{0z} \eta_{0r} - \hat{E}_{0r} \eta_{0z} \right) \frac{mJ_m^0}{\eta_{0r}\rho} \right] \hat{\mathbf{r}} \right. \\ &\quad \left. + \left[i \left(\hat{E}_{0z} \eta_{0r} - \hat{E}_{0r} \eta_{0z} \right) J_m'^0 - \hat{E}_{0\varphi_0} \eta_{0z} \frac{mJ_m^0}{\eta_{0r}\rho} \right] \hat{\varphi} + \hat{E}_{0\varphi_0} \eta_{0r} J_m^0 \hat{\mathbf{z}} \right\}\end{aligned}$$

8.2. Calculating the time-independent Poynting vector

Now that all the electric and magnetic field components for every mode and all regions (incident fields, scattered fields and blob fields), the Poynting vector can be easily calculated by using the well-known formula:

$$\tilde{\mathbf{s}} = \frac{1}{2} \text{Re}\{\tilde{\mathbf{e}} \times \tilde{\mathbf{h}}^*\}$$

The last equation is used to export all Poynting vector components for all waves and

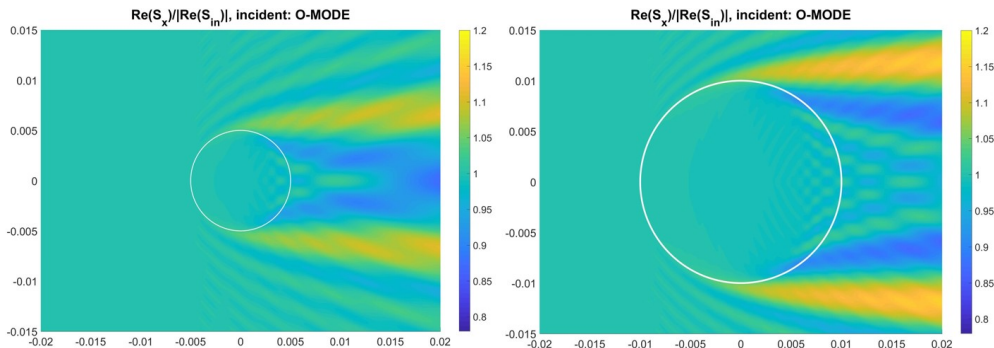


FIGURE 3. Poynting flux in the forward direction, frequency 170 GHz , blob radius 5 mm (left) and 10 mm (right), ambient density 10^{19} m^{-3} and blob density $1.5 \times 10^{19}\text{ m}^{-3}$, magnetic field inclination 0° , azimuth 0°

of course, is the one from which the numerical results are exported and plotted (in the next section).

9. Numerical results

By using the above formulas, one can achieve results for a variety of different scattering processes. In some cases, it is necessary to change the value of one only component while the others are kept the same, in order to easily understand the effect of each one of them on the radio frequency scattering.

9.1. The way the blob radius affects RF scattering

Starting with the blob radius, one way to study the effect of the length of the cylinder radius on the scattering process, is by plotting figures of the time-independent Poynting vector, especially of the component which points to the forward direction. Both presented (in the figure 3) cases refer to an ambient density of 10^{19} m^{-3} (left) and a blob density of $5.0 \times 10^{19}\text{ m}^{-3}$ (right), magnetic field inclination zero and azimuth of the incident wave in the cylinder coordinate system zero. It must be noted that the frequency of the RF wave has a major role in the scattering effects. The effects are different when the wavelength is of bigger, smaller or about the same size compared to the fluctuation. Figure 3 shows the Electron Cyclotron case, at 170 GHz , which has a wavelength of about 1.7 mm (smaller enough than the blob's dimensions). On the other hand, for the Low Hybrid waves at 4.6 GHz , the wavelength is much larger - about 6.5 cm , which is much bigger than the fluctuation's dimensions, too.

9.2. The way the blob density contrast affects RF scattering

Another interesting parameter for study, is the density contrast between the cylindrical filament and the background environment. The electrons density of the filament n_{fila} can be much different compared to the ambient electrons density n_{ambi} , so that the relative density contrast between the blob and the ambient electrons density can practically vary enough. A typical experimental range of values for $\delta n \equiv |n_{fila} - n_{ambi}|/n_{fila}$ is inside $(0.05, 1)$. In figure 4, there are two cases for the Electron Cyclotron waves at frequency 170 GHz for the same cylindrical blob radius, equal to 10 mm . There is neither magnetic field inclination with respect to the cylinder axis, nor azimuth taken into account. The left side is for ambient density 10^{19} m^{-3} and blob density $5.0 \times 10^{19}\text{ m}^{-3}$, while the right

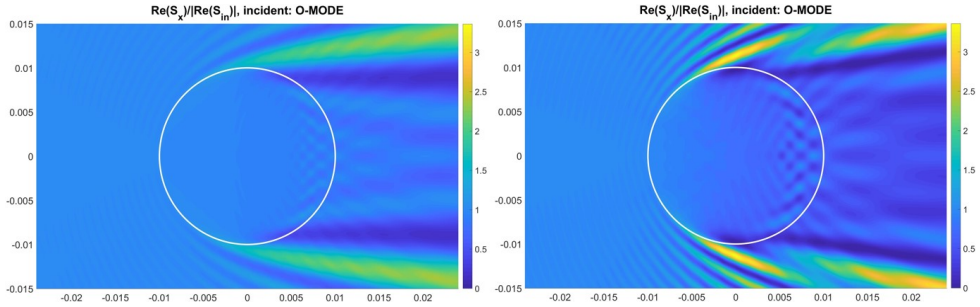


FIGURE 4. Poynting flux in the forward direction, frequency 170 GHz , blob radius 10 mm , ambient density 10^{19} m^{-3} and blob density $5.0 \times 10^{19}\text{ m}^{-3}$ (left) and $15 \times 10^{19}\text{ m}^{-3}$ (right), magnetic field inclination 0° , azimuth 0°

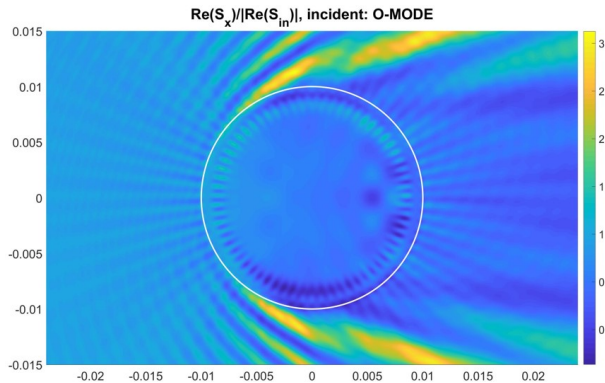


FIGURE 5. Poynting flux in the forward direction, frequency 170 GHz , blob radius 10 mm , ambient density $2.0 \times 10^{20}\text{ m}^{-3}$ and blob density $3.0 \times 10^{20}\text{ m}^{-3}$, magnetic field inclination 5° , azimuth 0°

side is for the same ambient density, but blob density is higher equal to $15 \times 10^{19}\text{ m}^{-3}$, so that the density contrast is different.

9.3. RF scattering with magnetic field inclination with respect to the cylinder axis

In figure 5, one can see the effect that the magnetic field inclination with respect to the cylinder axis has on the radiofrequency waves scattering. The magnetic field is chosen to be in angle of 5° with respect to the cylinder axis, while the chosen frequency of 170 GHz is referring again to the Electron Cyclotron waves case, the blob radius is equal to 10 mm , the ambient density is $2.0 \times 10^{20}\text{ m}^{-3}$ the blob density is $3.0 \times 10^{20}\text{ m}^{-3}$ and there is no azimuth taken into account.

9.4. The way the magnetic field inclination affects RF scattering for non-zero azimuth

The effect that the magnetic field inclination has on RF scattering, can also be studied in parallel with non-zero azimuth angle. So, in figure 6 the frequency is at 170 GHz (EC), the blob radius is equal to 10 mm , the ambient density is 10^{19} m^{-3} the blob density is $1.5 \times 10^{19}\text{ m}^{-3}$, the azimuth is 30° and the magnetic field inclination is 0° (left picture) and 30° (right picture).

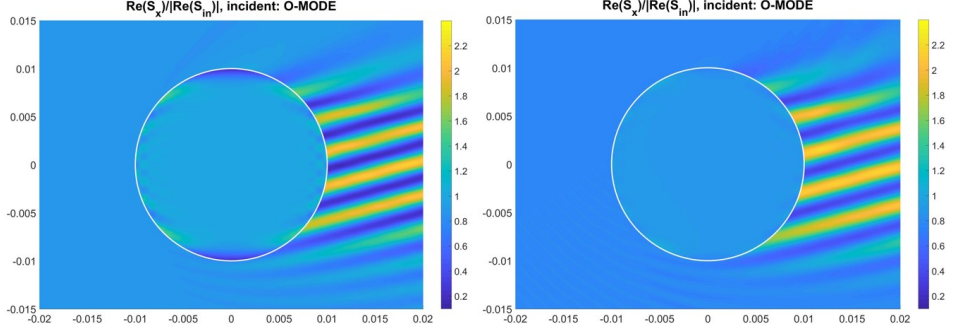


FIGURE 6. Poynting flux in the forward direction, frequency 170 GHz , blob radius 10 mm , ambient density 10^{19} m^{-3} and blob density $1.5 \times 10^{19}\text{ m}^{-3}$, magnetic field inclination 0° (left) and 30° (right), azimuth 30°

- RAM, A. K. & HIZANIDIS, K. 2016 Scattering of radio frequency waves by cylindrical density filaments in tokamak plasmas. *Physics of Plasmas* **23**, 022504-1–022504-17.
- IOANNIDIS, Z. C., RAM, A. K., HIZANIDIS, K. & TIGELIS, I. G. 2017 Computational studies on scattering of radio frequency waves by density filaments in fusion plasmas. *Physics of Plasmas* **24**, 102115-1–102115-13.
- RAM, A. K., HIZANIDIS, K. & KOMINIS, Y. 2013 Scattering of radio frequency waves by blobs in tokamak plasmas. *Physics of Plasmas* **20**, 056110-1–056110-10.
- STIX, T. H. 1992 Waves in plasmas. *New York, USA, American Institute of Physics*.